International Journal of Physical Sciences Vol. 7(23), pp. 2971-2979, 15 June, 2012
Available online at http://www.academicjournals.org/IJPS
DOI: 10.5897/IJPS12.219
ISSN 1992-1950 ©2012 Academic Journals

Full Length Research Paper

Effect of zinc acetate concentration on the structural and optical properties of ZnO thin films deposited by Sol-Gel method

M. Saleem[1], L. Fang1*, H. B. Ruan[1,2], F. Wu[1], Q. L. Huang[1], C. L. Xu[1] and C. Y. Kong[2]

[1]Department of Applied Physics, Chongqing University, Chongqing 400044, China.
[2]Optical Engineering Key Laboratory, Chongqing Normal University, Chongqing 400030, China.

Accepted 03 May, 2012

The transparent Zinc Oxide (ZnO) thin films were deposited by multi-step sol-gel method and the effect of sol concentration on structural, morphological and optical properties were investigated. X-ray diffraction (XRD) and scanning electron microscopy (SEM) were employed to characterize structures and morphologies of the as-deposited films. The crystallographic orientation of the ZnO films shows the preferred orientation of (002) that is along c-axis direction and the films were uniform and well adherent to the substrates. The grain size is in the range of 15.3~19.7 nm and the thickness in the range of 266~295 nm, both increase with zinc acetate concentration. It is found that the transmittance of the films is enhanced from 83 to 95% in the visible near- IR region in the range from 400 to 800 nm by increasing the concentration. The optical band gap energy attenuates from 3.307 to 3.227 eV and whereas the Urbach energies of the films increase from 68.2 to 82.4 meV with increasing the concentration from 0.35 M to 0.65 M.

Key words: Sol-Gel method, spin coating, structural properties, optical properties.

INTRODUCTION

Zinc oxide is a II-VI group, n-type semiconductor compound which has technical applications such as photocatalysts by Chakrabarti et al. (2004), solar cells by Pradhan et al. (2007) and Baxter et al. (2006), thin film gas sensors (Shishiyanu et al., 2005), varistors (Suvaci and Ozer 2005), light emitting diodes (Saito et al., 2002), spintronic devices (Meron and Markovich 2005), and nanolasers (Huang et al., 2001). ZnO thin films have also been widely used as surface acoustic wave (SAW) device and film bulk acoustic resonator (FBAR) because of its excellent piezoelectric properties by Webb et al. (1981) and Kang et al. (2005). Moreover, ZnO has large band gap 3.37 eV and large excitonic binding energy 60 meV at room temperature and its composed of hexagonal wurtzite crystal structure with lattice parameters a = 3.248Å and c = 5.205Å. ZnO thin film is applied as the transparent conductive film and the solar window because of the high optical transmittance in the visible light region.

Diverse techniques have been employed to fabricate ZnO thin film including RF sputtering (Tadatsugu et al., 1984), spray pyrolysis (Krunks and Mellikov 1995), metal-organic chemical vapour deposition (MOCVD) (Tominaga et al., 2002), molecular beam epitexy (MBE) (Look et al., 2002), pulsed laser deposition (PLD) (Naghavi et al., 2000) and the sol-gel process (Natsume and Sakata 2000; Luna-Arredondo et al., 2005; Farley et al., 2004; Mandalapu et al., 2006; Viart et al., 2003; Ohyama et al., 1997; Gonzalez et al., 1998). Sol-gel method has widely been adopted for the fabrication of transparent and conducting oxide due to its simplicity, safety, no need of costly vacuum system and hence cheap method for large area coating. The sol-gel process also offers other advantages such as high surface morphology at low crystallizing temperature, the easy control of chemical components and fabrication of thin films at low cost to investigate structural and optical properties of ZnO thin

*Corresponding author. E-mail: fangliangcqu@yahoo.com.cn. Tel: +86-23-65678369.

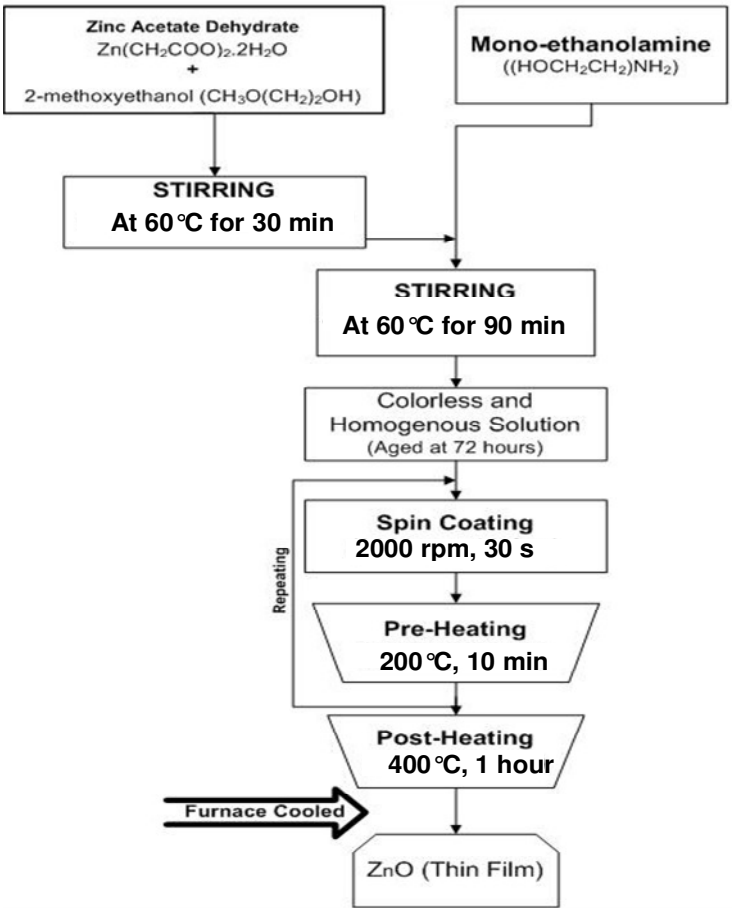

Figure 1. The flow chart showing the procedure for preparing ZnO films.

Film (Natsume and Sakata 2002). The deposition of doped and undoped ZnO thin films by using the sol-gel route has been already reported (Mandalapu et al., 2006; Viart et al., 2003; Ohyama et al., 1997; Gonzalez et al., 1998). However, up to date, multiple deposition steps (concentration of the sol-gel, heat treatment condition, substrates used etc.) have been generally necessary to produce high-quality thin films. Considering the afore-mentioned factors affecting the cost-of-ownership and the film quality aspects, a typical multi-step deposition process has been demonstrated.

In this article, we report growth of ZnO films with different zinc acetate concentrations on glass substrate by the sol-gel method using spin coating. The aim of this study is to investigate the influence of zinc acetate concentration on structural, morphological and optical properties.

MATERIALS AND METHODS

Chemicals

For the preparation of ZnO sol, following materials were used: Zinc acetate dehydrate [($Zn(CH_2COO)_2.2H_2O$), chemical purity 99.95%] (ZAD), 2-methoxyethanol [($CH_3O(CH_2)_2OH$), chemical purity 99.95%] (2-ME) and monoethanolamine [($(HOCH_2CH_2)NH_2$), chemical purity 99.95 %] (MEA).

ZnO sol-gel preparation

The sol-gel synthesis and thin film process is outlined in Figure 1. The final concentrations of ZAD were 0.35, 0.5 and 0.65 mol/L respectively, in 30 ml of 2-ME using 250 ml conical flask. After stirring for 30 min at 60°C, MEA was added drop wise under constant stirring. The resultant solutions were stirred for 90 min to yield colorless, homogeneous and transparent solutions. The solutions were aged for 72 h at room temperature in order to obtain the optimum viscosity during deposition of the film. The molar ratio of MEA to ZAD was maintained at 1:1. Prior to the coating of the film, the glass substrates were pre-cleaned with detergent, and then they were cleaned in methanol and acetone for 15 min each by using ultra-sonic water bath. Afterwards, substrates were rinsed with distilled water and then dried in hot air. The aged solution was dropped on glass substrates which were rotated at 2000 rpm for 30 s. The as- deposited films were then pre-heated at 200°C for 10 min into a furnace to evaporate the solvent and remove organic residuals. This spinning to preheating procedure was repeated eight times. After the deposition of final layer, films were post-heated in air at 400°C for 1 h in order to obtain crystallized ZnO in wurtzite structure. Well-oriented ZnO thin films can be controlled via adjusting the preparation parameters, such as precursor

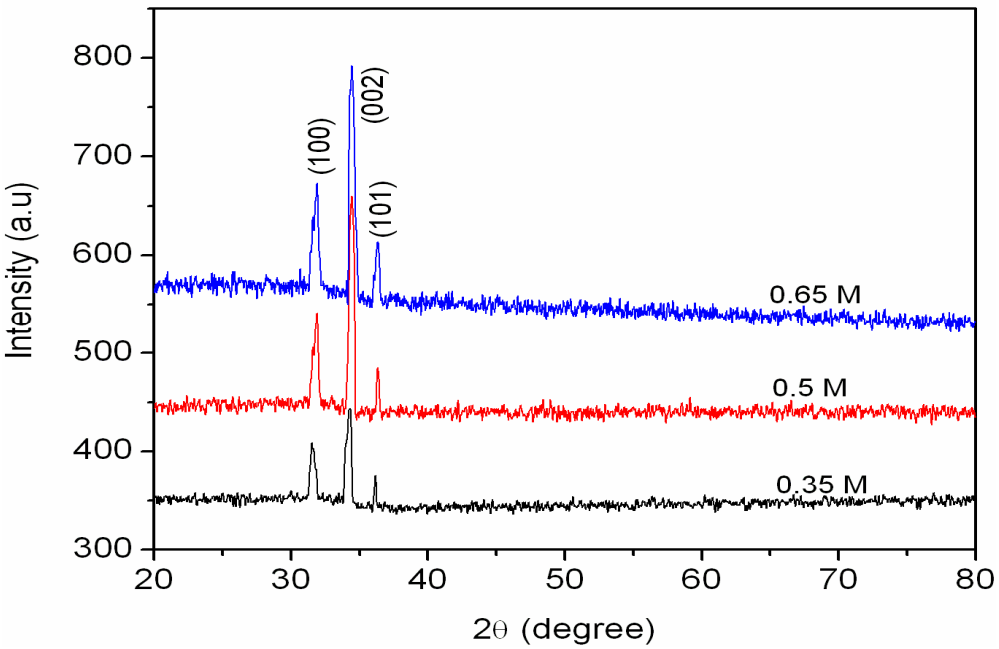

Figure 2. XRD spectra of the ZnO thin film with different content.

concentration, pre-heating and post- heating temperature and the sol aging time.

Material characterization

X-ray diffraction (XRD) was used for the crystalline structure of the ZnO thin films. XRD patterns were obtained with a MRD-Single Scan diffractometer with Cu Kα (λ=1.54056Å) radiation and scanning range of 2θ set between 20˚ and 80˚. During the measurement, the current and the voltage of XRD were maintained at 20 mA and 36 KV respectively, and scan speed was 4˚/min. The surface morphology of films was evaluated using Scanning Electron Microscopy (FEG-SEM, Nova-400). The thickness of the film was determined by a surface profilometer (AMBIOS).The transmission spectra of the films were recorded using a double-beam ultraviolet / visible (UV-4100) recording spectrophotometer with a wavelength range 200 to 800 nm and the optical band gap was measured from the transmission spectra.

RESULTS AND DISCUSSION

Structural analysis

Figure 2 shows the X-ray diffraction (XRD) patterns of ZnO films as a function of Zn content. It was observed that the as- deposited films were polycrystalline with hexagonal wourtzite structure. From the XRD patterns, (100), (002) and (101) diffraction peaks are observed showing the growth of ZnO crystallites in different directions. Strong preferential growth is observed along c-axis depending on the initial zinc concentration which is perpendicular to the surface of the substrate. By increasing the sol concentration, crystallinity of the samples ameliorates drastically, accompanying a strong reflex along c-axis that is, (002) plane. This result suggests that the sol concentration affects the films crystallinity as well as orientation of the crystallites in the films. The other orientations like (100) and (101) are also seen with comparatively lower intensities. It can be seen from Table 1 that the full width at half maximum (FWHM) of the (002) diffraction peak decreases when zinc concentration increases up to 0.65M, demonstrating that the crystalline quality of the film gets better as the concentration becomes higher. Wang et al. (2007) suggested the growth mechanism of c-axis oriented ZnO thin film is a self-assembly process in which a dipole-dipole interaction between the polar nanograins plays a great role for the crystal growth. They think that after the first layer of ZnO sol film was coated and pre-heated, the nuclei were formed and gradually grew into crystals. Since the glass substrate is an amorphous material, the nuclei should be randomly oriented; correspondingly, the crystals were also randomly oriented. However, the (002) plane of ZnO has the minimum surface energy (Fujimura et al., 1993) so most of the crystals grew preferentially along the (002) direction and only a small part of crystals grew along other directions. After the second layer of ZnO sol film was coated and pre-heated, the new crystals were formed using the former layer as a growth template; therefore, some new crystals still grew along other directions rather than the (002) direction and so on. This process can explain why sample has the (100) and (101) peaks besides the (002) peak. However, the XRD results in the present study indicate that all the films are polycrystalline and randomly oriented. Although

Table 1. Structural parameters of ZnO thin films.

Zinc content (mol/L)	Planes	2θ (degrees)	d (Å)	I/I_0	FWHM (degrees)
0.35	100	31.64	2.8255	48.1	0.523
	002	34.31	2.6115	100	0.539
	101	36.17	2.4813	45.2	0.369
0.5	100	31.789	2.8126	19.9	0.525
	002	34.22	2.6181	100	0.493
	101	36.27	2.4747	19.3	0.351
0.65	100	31.9	2.8031	41.9	0.411
	002	34.45	2.6012	100	0.417
	101	36.36	2.4688	32.9	0.392

Table 2. Evaluated structural parameters of ZnO thin films.

Zinc content (mol/L)	Planes	FWHM(β)˚	2θ˚	D (nm)	$\delta \times 10^{-3}$ $(nm)^{-2}$	Strain (%)	Eg (eV)	Eu (meV)	Thickness (nm)
0.35	002	0.539	34.31	15.3	4.3	0.346	3.307	68.2	266
0.5	002	0.493	34.22	16.9	3.5	0.599	3.303	77.5	285
0.65	002	0.417	34.45	19.7	2.5	-0.05	3.227	82.4	295

Ohyama et al. (1998) and Natsum et al. (2000) reported c-axis that is (002) plane oriented ZnO films on glass substrate, the random orientation in this study is due to the difference in the precursor chemistry and pre- and pos-heating temperatures (Fujihara et al., 2001). The structural parameters of ZnO thin films obtained form the XRD patterns are presented in Table 1.

From the XRD spectrum, grain size (D) of the films is calculated using the Debye Scherrer formula by Khan et al. (2010).

$$D = k\lambda / \beta \cos\theta \quad (1)$$

where k is a constant to be taken as 0.49 and λ, β, and θ are the X-ray wavelength (=1.5406Å), full width at half maximum (FWHM) and Bragg angle respectively. By inserting different values from Table 1 in the Scherrer formula, grain sizes of (002) oriented thin films obtained is presented in Table 2. The calculated values of the grain size ranged between 15.4 and 19.8 nm which are approximately same as found in the literature by Kumari et al. (2011). It was observed that grain size increased with increasing zinc concentration. This trend agrees well with SEM micrograph analysis shown in Figure 4, where the ZnO grain size is clearly seen to increase with increasing Zn concentration.

The dislocation density (δ), defined as the length of dislocation lines per unit volume of the crystal is calculated using the following formula by Khan et al. (2010).

$$\delta = 1/D^2 \quad (2)$$

Strain (ε_{zz}) of the thin films is calculated from the c-axis lattice parameter using the following formula by Ong et al. (2002).

Where, c is the lattice parameter of ZnO films calculated from XRD data and c_o = 5.205Å is the unstrained lattice parameter of ZnO. According to the above formula, the positive values of ε_{zz} represent tensile strain while a negative value represents compressive strain. As the ZnO

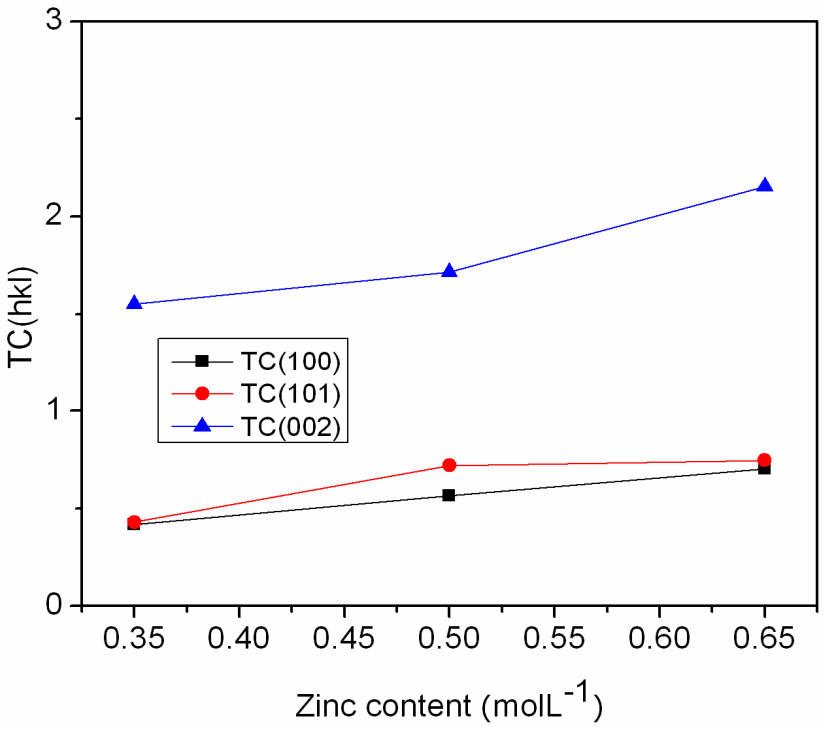

Figure 3. Variation of TC(hkl) values of ZnO films with zinc content.

$$\varepsilon_{zz} = \frac{c - c_o}{c_o} \times 100\% \quad (3)$$

content increases the thickness of the film also increases, indicating that as the film grows thicker, the film is relaxed by reducing the strain. The film which has thickness 295 nm shows the minimum strain. The evaluated structural parameters of ZnO thin films using its (002) reflection are presented in Table 2, showing that the strain in sol-gel derived ZnO films is tensile and the optimum thickness of film could be up to around 300 nm for the best structural quality. According to Ghosh et al. (2004), the tensile strain might be due to a thermal mismatch between the ZnO film and glass substrate. From the dislocation density data, one can clearly observe that the crystallization of the films is good because of their small dislocation density (δ) values which represent the amount of defects in the film. The larger D and smaller full width at half maximum (FWHM) values show better crystallization of the films.

Moreover the texture coefficient TC (hkl) is introduced to characterize the preferential crystallite orientation along the (hkl) direction defined by Manifacier et al. (1976).

$$TC(hkl) = \frac{I(hkl)/I_o(hkl)}{N^{-1}\sum_N I(hkl)/I_o(hkl)} \quad (4)$$

Where I(hkl), I_O(hkl) and N are the measured relative intensity of a diffraction peak, intensity of the standard powder diffraction peak and the number of diffraction peaks respectively. If TC (hkl) = 1, for all the (hkl) planes considered, indicates a sample with randomly oriented crystallite, while values larger than 1, indicate the abundance of crystallite in a given (hkl) direction. Values 1> TC (hkl) >0 indicate the lack of grains orientated in that direction. The TC (hkl) values calculated for the three main diffraction peaks that is (100), (002) and (101) are given in Figure 3. It can be observed that the highest TC(hkl) value is in (002) plane for all ZnO thin films.

Morphological analysis

Scanning electron microscopy (SEM) micrograph of ZnO thin films are shown in Figure 4 and the films show large number of grain boundaries. It can be seen from Figure 4 that grains become more uniform and bigger in size as the sol-gel zinc content increases and the small grains made a smooth surface with a fine structure similar to those observed by Kumari et al. (2011). This can be understood from the XRD results. The thickness measurement data of ZnO thin films are also presented in Table 2. It was observed that increasing zinc concentration of prepared sol resulted in an increase in film thickness from 266 to 295 nm which can be explained as follows. As the concentration of solution increases, film

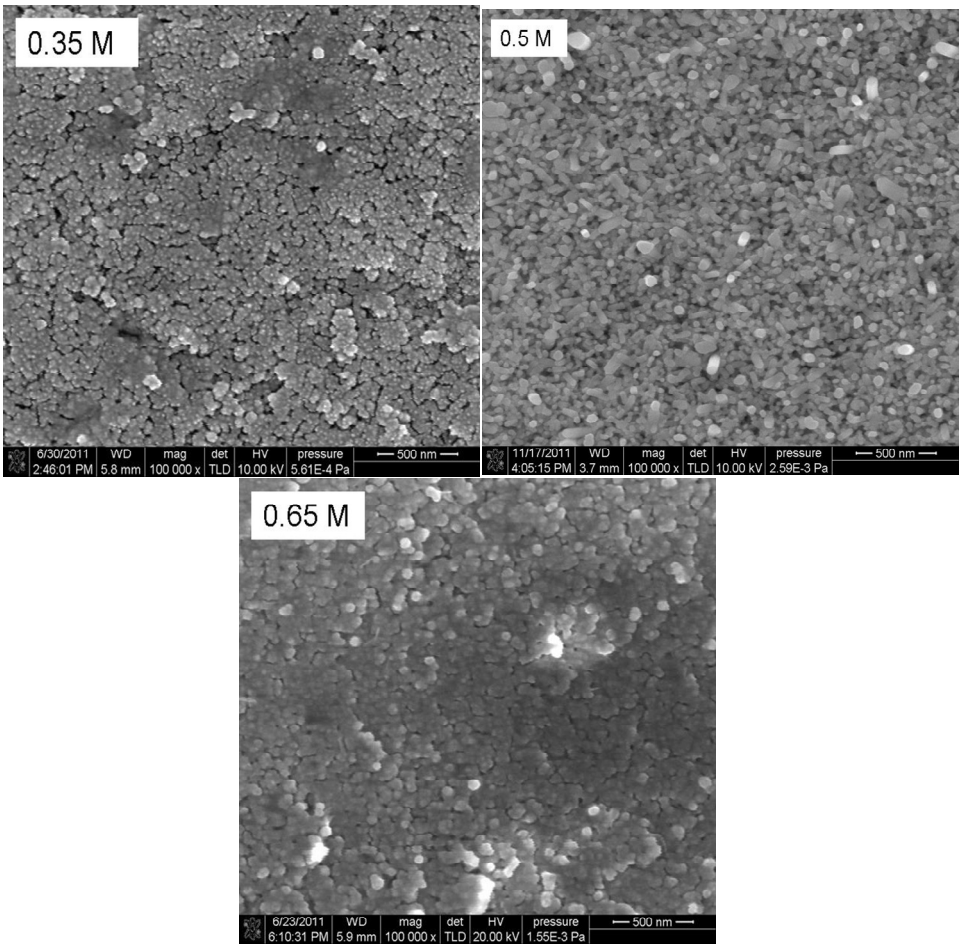

Figure 4. The SEM morphology of ZnO thin films with different content.

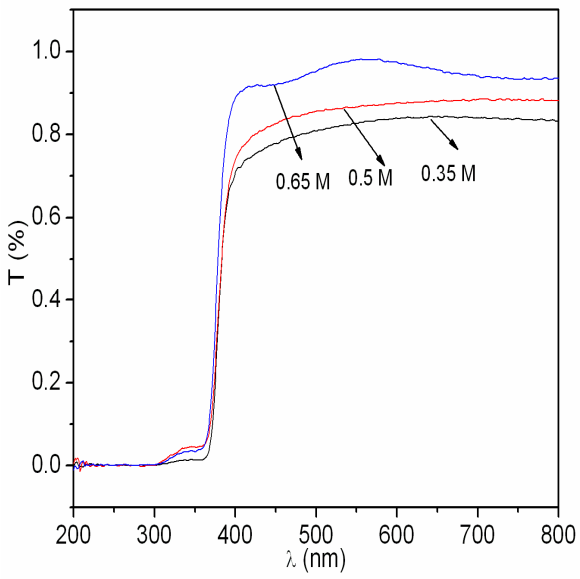

Figure 5. Transmittance spectra of ZnO film with different content.

growth increases, which in turn, increase the film thickness and the grain size. However, considerable micropores related to the grain boundaries are observed as the film grows thicker. Studies by Brinker and Scherer, (1975) have shown that the micro and nanopores are usual characteristics of sol-gel derived ZnO film.

Optical properties

Figure 5 depicts the optical transmittance spectra of sol-gel deposited ZnO thin films in the UV-visible region from 200 to 800 nm. The transmittance was 83 to 95% in the visible- near IR region from 400 to 800 nm for ZnO concentration from 0.35 to 0.65 M. It is found that the transmittance increases with a decrease in solution concentration. However, the larger transmittance in 0.5 and 0.65 M concentration may be due to the structural homogeneity and crystallinity as evidenced from Figure 4. The transmittance of the films increases with the increase of ZnO concentration as shown in the study of Kim et al. (2005), who suggested that the transmittance of the films

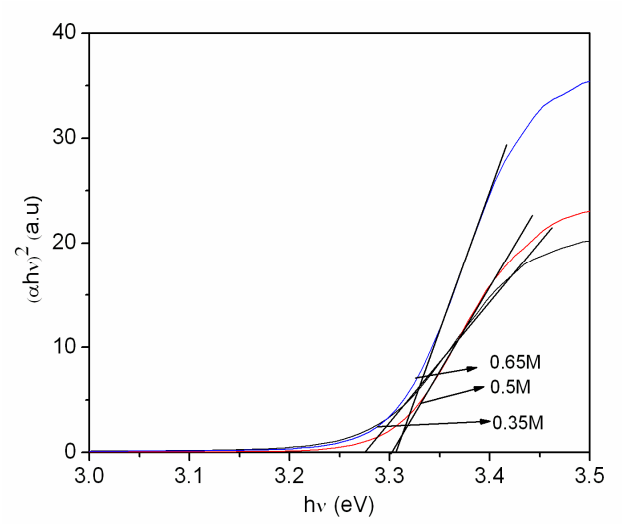

Figure 6. Plot of $(\alpha hu)^2$ vs. photon energy (hu) of ZnO film with different content.

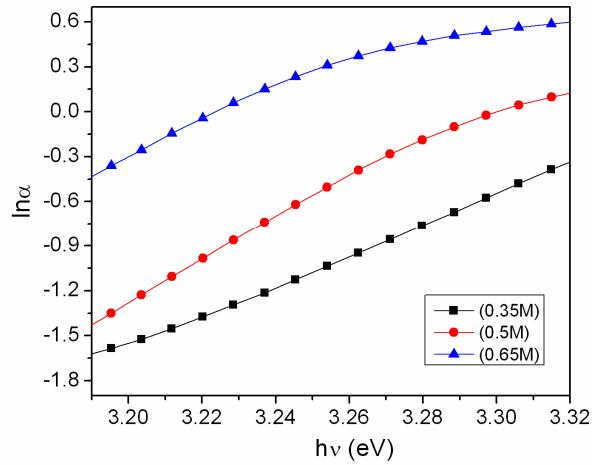

Figure 7. The plot of ln(α) vs. photon energy (hu) of ZnO thin film.

increases with the percentage of c-axis orientation, consistent with a reduction in light dispersion in grain boundaries as the film microstructure becomes more c-axis oriented. The results indicate that high optical quality ZnO thin films can be successfully achieved via this low temperature chemical approach. In the visible region of solar spectrum, transmission spectrum of 0.65 M film show sinusoidal behavior; this may be due to the layered structure of thin film. The corresponding optical band gap of ZnO thin films is estimated by extrapolation of the linear relationship between $(\alpha hu)^2$ and hu according to the equation given by Caglar et al. (2009).

$$(\alpha hu)^2 = A\,(hu - Eg) \quad (7)$$

Where α is the absorption coefficient, hu is the photon energy, Eg is the optical band gap and A is a constant. Figure 6 depict the plot of $(\alpha hu)^2$ versus photon energy hu. Extrapolation of linear portion to the energy axis gives the band gap energy (Eg). The estimated values of Eg are listed in Table 2. The band gap values of ZnO thin films are found to be 3.307eV to 3.227eV with the increase of ZnO content. The band gap of ZnO films decreases nearly linearly that can be explained with the increase in crystallinity and the grain size factors. The decrease in band gap has also been observed by Zelaya-Angel et al. (1994) for CdS films. Therefore, our results are in good agreement with the reported values in literature (Lokhande et al., 2002; Lee et al., 1996). Furthermore, band gap lowering can occur due to the presence of defect states, disorder etc. However, such defects will produce tail in the transmittance spectra which are clearly observed in the present study (Figure 5).

For many materials, it is assumed that the absorption coefficient α near the band edge shows an exponential dependence on photon energy hu. This dependence is given by the relation obtained from Urbach (1953).

$$\alpha = \alpha_o \exp [hu/Eu] \quad (8)$$

Where α_o is a constant and Eu is Urbach energy which is the width of the tails of the localized states associated with the amorphous state in the forbidden gap. The logarithm of the absorption coefficient α versus photon energy hu is shown in Figure 7. The value of Eu is calculated by taking the reciprocal of the slope of the linear portion in the lower photon energy region and the values obtained from this figure are given in Table 2. The Eu values change inversely with optical band gape energy. Ziaul et al. (2010) and Caglar et al. (2009) have reported approximately same results for the Urbach energy. The Urbach tail (Eu) is used to describe exponential dependence of the absorption coefficient at the optical absorption edge. The change of Urbach tail (Eu) is caused by disorder in the materials, which leads to an extension of the parabolic density of states into the band edge. Disorder generally includes thermal disorder, which reflects thermal occupation of phonon states, or structural disorder, which is associated with impurities and defects in the material (Cody et al., 1981). In this case, the Urbach tail was mainly attributed to the effects of solution concentration on the fundamental optical absorption.

Conclusion

In this study, we have grown transparent ZnO thin films on glass substrate by a multi-step sol-gel technique with 0.35 to 0.65 M zinc acetate concentrations solution. The structural, morphological and optical properties were investigated. It is found that the structural and optical

properties were largely improved by changing sol-gel molar concentration.

1. According to XRD results, the as-deposited films exhibited a hexagonal wurtzite structure with (002) preferential orientation after annealing at 400˚C in air ambiance for 1 h.
2. The grain size and the thickness of the films are found to depend on sol-gel concentration and increase from 15.3 to 19.7 nm and 266 to 295 nm when the sol concentration changes from 0.35 M to 0.65 M, respectively.
3. SEM micrograph of ZnO thin film shows that the grain become more uniform and bigger in size and the small grains made a smooth surface with a fine structure.
4. The average transmittance of the samples are 83 to 95% in the visible wavelength range from 400 to 800 nm while band gap and Urbach energies are found to be 3.307 to 3.227 eV and 68.2 to 82.4 meV when the sol concentration changes from 0.35 to 0.65 M.

ACKNOWLEDGEMENTS

This work was supported by the Fundamental Research Fund for the Central Universities No. CDJXS10102207, the National Natural Science Foundation of China (Grant Nos. 11075314 and 50942021) and Natural Science Foundation of Chongqing City under Grant CSTC, 2011BA4031, the Third Stage of “211” Innovative Talent Training Project (No.S-09109) and the Sharing Fund of Large-scale Equipment of Chongqing University (Grant Nos. 2011121556, 2010121556).

REFERENCES

Baxter JB, Aydil ES (2006). Dye-sensitized solar cells based on semiconductor morphologies with ZnO nanowires. Sol. Energy Mater, Sol. Cells, 90: 607-622.
Brinker CJ, Scherer GW (1975). The Physics and Chemistry of Sol-Gel Processing. Academic Press, New York. Sol-Gel Sci., pp. 87-92.
Caglar M, Ilican S, Caglar Y (2009). Influence of Dopant Concentration on the Optical Properties of ZnO: In films by Sol-Gel Method. Thin Solid Films, 517(17): 5023-5028.
Chakrabarti S and Dutta BK (2004). Photocatalytic Degradation of Model Textile Dyes in Wastewater Using ZnO as Semiconductor Catalyst. J. Hazard. Mater., 112(3): 269-278.
Cody GD, Tiedje T, Abeles B, Brooks B, Goldstein Y (1981). Theoretical study of the optical absorption edge in Amorphous Semiconductors. Phys. Rev. Lett., 47: 1480-1486.
Farley NRS, Staddon CR, Zhao LX, Ed- munds KW, Gallagher BL, Gregory DH (2004). Sol-Gel Formation of Ordered Nanostructured Doped ZnO Films. J. of Materials Chem., 14(7): 1087-1092.
Fujihara S, Sasaki C, Kimura T (2001). Crystallization behavior and origin of c-axis orientation in sol-gel derived ZnO: Li thin films on glass substrates. Appl. Surf. Sci., 180: 341-350.
Fujimura N, Nishihara T, Goto S, Xu J, Ito T (1993). Control of preferred orientation for ZnO_X films: control of self-texture. J. Cryst. Growth, 130: 269-279.
Ghosh R, Basak D, Fujihara S (2004). Effect of substrate-induced strain on the structural, optical and electrical properties of polycrystalline ZnO thin films. J. Appl. Phys., 96: 2689-2692.
Gonzalez EJ, Urueta JAS, Parra RS (1998). Optical and Electrical Characteristics of Aluminum-Doped ZnO Thin Films Prepared by Sol-Gel Technique. J. Crystal Growth, 192(3-4): 430-438.
Huang MH, Mao S, Feick H, Yan H, Wu Y, Kind H, Weber E, Russo R, Yang P (2001). Room-Temperature Ultraviolet Nanowire Nanolasers. Science, 292(5523): 1897-1899.
Kang SJ, Choi JY, Chang DH, Yoon YS (2005). A Study on the Growth and Piezoelectric Characteristics of ZnO Thin Film Using a RF Magnetron Sputtering Method. J. Korean Phys. Soc., 47(93): 589-594.
Khan ZR, Zulfequar M, Khan MS (2010). Optical and Structural Properties of Thermally Evaporated Cadmium Sulphide Thin Films on Silicon (100) Wafers. Mater. Sci. Eng. B, 174(1-3): 145-149.
Kim YS, Tai WP, Shu SJ (2005). Effect of preheating temperature on structural and optical properties of ZnO thin films by sol-gel process. Thin Solid Films, 491: 153-160.
Krunks M, Mellikov E (1995). Zinc Oxide Thin Films by the Spray Pyrolysis Method. Thin Solid Film. 270 (1-2): 33-36.
Kumari V, Kumar V, Malik BP, Mohan D, Mehra RM (2011). Laser Induced Nonlinear Optical Properties of Zinc Oxide Thin Film Prepared. J. of Nano- and Electronic Phys., 3(1): 601-609.
Lee CH, Lin LY (1996). Characteristics of spray pyrolytic ZnO thin films. Appl. Surf. Sci., 92: 163-166.
Lokhande BJ, Patil PS, Uplane MD (2002). Deposition of highly oriented ZnO films by spray pyrolysis and their structural, optical and electrical characterization. Mater. Lett., 57: 573-579.
Look DC, Reynolds DC, Litton CW, Jones RL, Eason DB, Gantwell G (2002). Characterization of Homo- epitaxial p-Type ZnO Grown by Molecular Beam Epitaxy. Appl. Phys. Lett., 81(10): 1830-1832.
Luna-Arredondo EJ, Maldonado A, Asomoza R, Acosta DR, Melendez-Lira MA, de la L, Olvera M (2005). Indium-Doped ZnO Thin Films Deposited by the Sol- Gel Technique. Thin Solid Films, 490(2): 132-136.
Mandalapu LJ, Xiu FX, Yang Z, Zhao DT, Liu JL (2006). P-Type Behavior from Sb-Doped ZnO Heterojunction Photodiodes. Appl. Phys. Lett., 88(11): 112108-112110.
Manifacier JC, Gasiot J, Fillard JP (1976). A simple method for the determination of optical constants n, k and the thickness of weakly absorbing thin film. J. Phys. E, 9: 1002-1011.
Meron T, Markovich G (2005). Ferromagnetism in Colloidal Mn^{2+}-Doped ZnO Nanocrystals. J. Phys. Chem. B, 109(43): 20232-20236.
Naghavi N, Marcel C, Dupont L, Rougier A, Leriche JB, Guery C (2000). Structural and Physical Characterization Of transparent Conducting Pulsed Laser Deposited In2O3-ZnO Thin Films. J. Mater. Chem., 10(10): 2315-2319.
Natsume Y, Sakata H (2000). Zinc oxide films prepared by sol-gel spin-coating. Thin solid films, 372: 30-36.
Natsume Y, Sakata H (2002). Electrical and Optical Properties of Zinc Oxide Films Post-Annealed in H2 after Fabrication by Sol-Gel Process. Mat. Che. and Phys., 78(1): 170-176.
Ohyama M, Kozuka H, Yoko T (1997). Sol-Gel Preparation of ZnO Films with Extremely Preferred Orientation along (002) Plane from Zinc Acetate Solution. Thin Solid Films, 306(1): 78-85.
Ohyama M, Kozuka H, Yoko T (1998). Sol-Gel Preparation of Transparent and Conductive Aluminum-doped ZnO films with highly preferential crystal orientation. J. Am. Ceram. Soc., 81(6): 1622-1632.
Ong HC, Zhu AXE, Du GT (2002). Dependence of the exitonic transition energies and mosaicity on residual strain in ZnO thin films. J. Appl. Phys. Lett., 80: 941-948.
Pradhan B, Batabyal SK, Pal AJ (2007). Vertically aligned ZnO nanowire arrays in Rose Bengal-based dye- sensitized solar cell. Sol. Energy Mater. Sol. Cells, 91: 769-773.
Saito N, Haneda H, Sekiguchi T, Ohashi N, Sakagu- chi I, Koumoto K (2002). Low-Temperature Fabrication of Light-Emitting Zinc Oxide Micropatterns Using Self-As- sembled Monolayers. Adv. Mater., 14(6): 418-421.
Shishiyanu ST, Shishiyanu TS, Lupen OI (2005). Sensing Characteristics of Tin-Doped ZnO Thin Films as NO2 Gas Sensor. Sensors and Actuators B: Chem., 107(1): 379-386.
Suvaci E, Ozer IO (2005). Processing of Textured Zinc Oxide Varistors via Templated Grain Growth. J. Eur. Ceram. Soc., 25(9): 1663-1673.
Tadatsugu M, Hidehito N, Shinzo T (1984). Zinc oxide thin film

ammonia gas sensors with high sensitivity and excellent selectivity. J. Appl. Phys., 23(5): 280-286.
Tominaga K, Takao T, Fukushima A, Moriga T, Nakabayashi I (2002). Amorphous ZnO-In2O3 Transparent Conductive Films by Simultaneous Sputtering Method of ZnO and In2O3 Targets. Vacuum, 66(3-4): 505-509.
Urbach F (1953). The long-wavelength edge of the photographic sensitivity and of the electronic absoption of solids. Phys. Rev., 92: 1324.
Viart N, Richard-Plouet M, Muller D, Pourroy G (2003). Synthesis and Characterization of Co/ZnO Nanocomposites: Towards New Perspectives Offered by Metal/Piezoelectric Composite Materials. Thin Solid Films, 437(1-2): 1-9.
Wang J, Qi Y, Zhi Z, Guo J, Li M, Zhang Y (2007). Growth mode of sol-gel derived PLT seeding layers on glass substrates and its effects on templating the oriented growth of PLZT thin film. Smart Mater. Struct., 16: 2673-2679.
Webb JB, Williams DF, Buchanan M (1981). Transparent and Highly Conductive Films of ZnO Prepared by RF Reactive Magnetron Sputtering. Appl. Phys. Lett., 39(8): 640-642.
Zelaya-Angel O, Alvarado-Gil JJ, Lozada-Morales R, Varges H, Ferreira da Silva A (1994). Band-gap shifts in CdS semiconductors by photoacoustic spectroscopy. Appl. Phys. Lett., 64(3): 291-298.